

## Synthesis, Structure, and Dynamic Properties of $[\text{Ni}_2\text{Sn}_{17}]^{4-}$

Emren N. Esenturk, James C. Fettinger, and Bryan W. Eichhorn\*

Department of Chemistry and Biochemistry, University of Maryland, College Park, Maryland 20742

Received August 6, 2005; E-mail: eichhorn@umd.edu

The synthesis, structure, and properties of bimetallic alloy and core-shell nanoparticles (NPs) are of interest due to their unusual catalytic, optical, and magnetic properties. Synthetic methods continue to be developed for the preparation of uniform, relatively monodispersed bimetallic particles in increasingly smaller size ranges (1–5 nm size regime) for a number of bimetallic systems.<sup>1,2</sup> An alternative approach to study bimetallic NPs involves the preparation of increasingly large molecular bimetallic clusters that approach or achieve bulk alloy structures.<sup>3–6</sup> These systems often rely on tightly bound ligand shells that help define a fixed nuclearity with rigorous monodispersity and minimal disorder in the crystal lattice. While the ligand spheres can alter or eliminate the reactivity and properties of the nanoparticle core, the ligated clusters are more amenable to structural and spectroscopic characterization and provide valuable insight into the makeup of bimetallic NP architectures.

Transition metal derivatives of the polyatomic main group anions (Zintl ions) bridge the chemistry of large clusters and NPs.<sup>7,8</sup> For example, the highly symmetric ligand-free  $[\text{M}@\text{Pb}_{12}]^{2-}$  icosahedral anions ( $\text{M} = \text{Pt}, \text{Pd}, \text{Ni}$ ) are the smallest possible subunit in a NP closest packed crystal lattice and are models for core-shell structures without ligand spheres.<sup>9,10</sup> In addition to having interesting electronic and spectroscopic properties, the molecular nature of these clusters allows for the study of solution dynamics by way of dynamic multinuclear NMR spectroscopy. The asymmetric nature of the  $[\text{Ni}@\text{Pb}_{10}]^{2-}$  bicapped square antiprismatic cluster showed that intramolecular exchange of the equatorial and capping Pb atoms is fast on the NMR time scale at very low temperatures.<sup>11</sup> Other “single focus” clusters (i.e., those having one centered atom) show similar fluxionality,<sup>15</sup> suggesting that many small metallic particles have extensive atomic mobility. The recent report<sup>12,13</sup> of the two-focus clusters,  $[\text{Pd}_2@\text{Ge}_{18}]^{4-}$  and  $[\text{Ni}_3@\text{Ge}_{18}]^{4-}$ , raises the question of whether atomic exchange can occur in larger, more separated regions of clusters and NPs. We report here the synthesis, characterization, and surprising dynamic exchange in  $[\text{Ni}_2\text{Sn}_{17}]^{4-}$ : a two-focus cluster with  $\text{NiSn}_8$  subunits linked by a single Sn atom.

Ethylenediamine (en) solutions of  $\text{K}_4\text{Sn}_9$  react with toluene solutions of  $\text{Ni}(\text{COD})_2$  in the presence of 2,2,2-crypt to give the  $[\text{Ni}_2\text{Sn}_{17}]^{4-}$  ion, **1**, in ca. 20% crystalline yield as the  $[\text{K}(2,2,2\text{-crypt})]^+$  salt.<sup>14</sup> The anion results from oxidation of the starting materials, which is facilitated by reduction of en solvent molecules and subsequent  $\text{H}_2$  elimination. The generated  $\text{H}_2$  is trapped through the hydrogenation of COD ligands and results in the formation of cyclooctene (GC–MS analysis). The reaction is similar to the  $\text{H}_2$  formation in the synthesis<sup>15</sup> of  $[\text{Sn}_9\text{Pt}_2(\text{PPh}_3)]^{2-}$ , and the proposed balanced equation is summarized in eq 1.

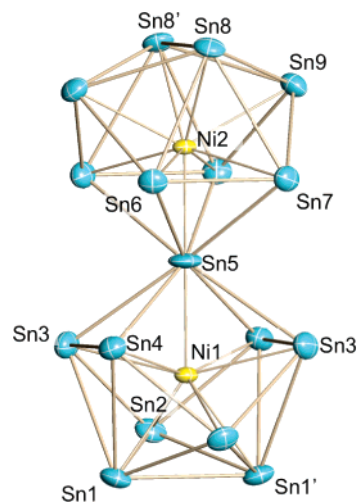
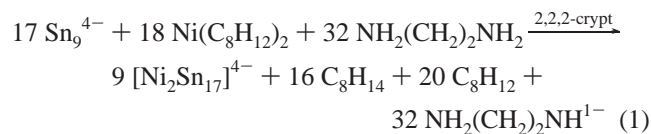
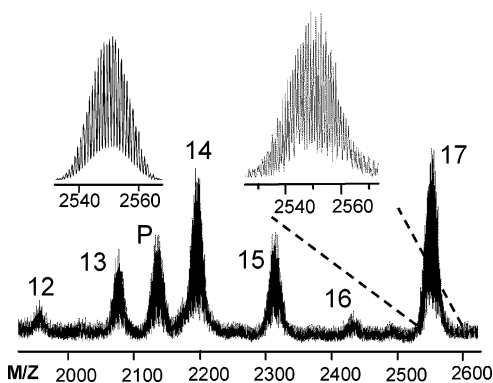


Figure 1. ORTEP drawing of the  $[\text{Ni}_2\text{Sn}_{17}]^{4-}$  ion.

The crystalline salt is dark red–brown and dissolves in dimethyl formamide (dmf), acetonitrile ( $\text{CH}_3\text{CN}$ ), and dimethyl sulfoxide (dmsO) to form dark red–brown solutions. The complex is air and moisture sensitive in solution and in the solid state. The salt has been characterized by single-crystal X-ray diffraction, energy dispersive X-ray analysis (EDX),  $^{119}\text{Sn}$  NMR spectroscopy, and electrospray ionization mass spectrometry (ESI-MS).

$[\text{K}(2,2,2\text{-crypt})]_4[\text{Ni}_2\text{Sn}_{17}]$  salt crystallizes in the monoclinic system, space group  $I2/a$ , with an ethylenediamine solvate molecule in the crystal lattice.<sup>16</sup> The  $[\text{Ni}_2\text{Sn}_{17}]^{4-}$  anion (Figure 1) possesses crystallographic  $C_2$  symmetry but has virtual  $D_{2d}$  point symmetry with a mirror plane defined by Sn8, Sn5, Sn2. The anion has 17 Sn vertices and two interstitial Ni atoms. The structure can be viewed as two coupled  $\text{Ni}@\text{Sn}_9^{2-}$  clusters that share a common vertex (Sn5). The  $\text{Ni}@\text{Sn}_9^{2-}$  subunits are quite similar to the  $C_{3v}$  structures of related  $[\text{M}@\text{E}_9\text{M}(\text{PPh}_3)]^{2-}$  clusters ( $\text{M} = \text{Ni}, \text{E} = \text{Ge}; \text{M} = \text{Pt}, \text{E} = \text{Sn}$ )<sup>15,17</sup> but differs from the  $C_{4v}$  structure of  $[\text{Ni}@\text{Sn}_9\text{Ni}(\text{CO})]^{3-}$ . Each  $\text{Ni}@\text{Sn}_9^{2-}$  subunit is a 20 electron,  $2n + 2$  cluster and should adopt a *closo*-type architecture according to Wades rules. However, they do not show the expected deltahedral geometry and violate Wades predictions, which is not uncommon among centered Zintl anions (i.e.,  $[\text{Sn}_9\text{Pt}_2(\text{PPh}_3)]^{2-}$  and  $[\text{Ge}_9\text{Ni}_2(\text{PPh}_3)]^{2-}$  complexes).<sup>15,17</sup>

Excluding the distances to Sn5, the Sn–Sn contacts within the cluster average 3.05(8) Å and are similar to other tin complexes (e.g.,  $[\text{Ni}@\text{Sn}_9\text{Ni}(\text{CO})]^{3-}$ ,  $[\text{Sn}_9\text{Cr}(\text{CO})_3]^{4-}$ ,  $[\text{Sn}_6\{\text{Cr}(\text{CO})_5\}_6]^{2-}$ ).<sup>15,18–20</sup> The shared vertex Sn5 is in an unusual pseudo-cubic  $\text{Sn}_8$  coordination environment with slightly longer Sn–Sn contacts of 3.133 Å, *av*. The long contacts to Sn5 are due to its high coordination number that is more akin to solid-state compounds. For example,  $\text{BaSn}_5$  has a central Sn atom with 12 nearest neighbors at 3.437 Å.<sup>21</sup> The Ni–Sn5 distances are shorter (2.384(3) Å, *av*) than other 16 Ni–Sn contacts in the anion (2.68(4) Å, *av*), indicating compression of the cluster along the Ni2–Sn5–Ni1 vector. The latter distances



**Figure 2.** Negative ion ESI mass spectrum of  $[K(2,2,2\text{-crypt})]_4[Ni_2Sn_{17}]$ . The labels represent the number of Sn atom ( $n$ ) in the  $[K(2,2,2\text{-crypt})Ni_2Sn_n]^{1-}$  series of ions. P is the oxidized  $[Ni_2Sn_{17}]^{1-}$  parent ion. The insets show the  $[K(2,2,2\text{-crypt})Ni_2Sn_{17}]^{1-}$  peak and its simulated pattern.

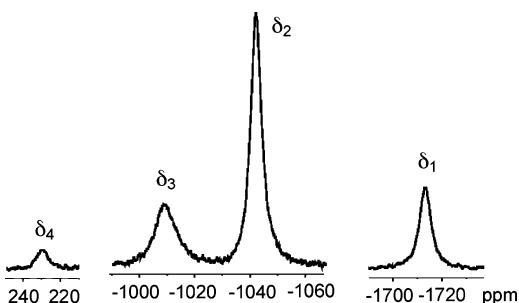


**Figure 3.**  $^{119}\text{Sn}$  NMR spectrum of the  $[Ni_2Sn_{17}]^{2-}$  ion recorded in dmf at  $-64\text{ }^\circ\text{C}$ . Peaks are plotted on the same intensity scale.

are similar to those of  $[Ni@Sn_9Ni(CO)]^{3-}$  (2.619(4) and 2.681(2) Å) and the predicted distances in  $[Ni@Sn_{10}]^{2-}$  (2.61–2.93 Å).<sup>15,22</sup>

The electrospray mass spectrum of **1** was recorded in the negative ion mode from dmf solutions of a crystalline  $[K(2,2,2\text{-crypt})]_4[Ni_2Sn_{17}]$  sample. The spectrum (Figure 2) shows the oxidized molecular ion,  $[Ni_2Sn_{17}]^{1-}$  (peak P), as well as a strong signal of the  $[K(2,2,2\text{-crypt})]^+$ -coordinated molecular ion (peak 17). An enlarged view of this peak showing its distinctive mass envelope and simulated pattern is shown in the insets. The spectrum also shows the sequential degradation products of **1**,  $[K(2,2,2\text{-crypt})Ni_2Sn_n]^{1-}$ , where  $n = 16\text{--}12$ , due to systematic loss of Sn atoms. This phenomenon was also observed<sup>23</sup> in the gas-phase degradation of  $[As@Ni_{12}@As_{20}]^{3-}$  and illustrates the ability of these clusters to fragment and renucleate in alternative structures.

The low-temperature limiting  $^{119}\text{Sn}$  NMR spectrum of  $[Ni_2Sn_{17}]^{4-}$  at  $-64\text{ }^\circ\text{C}$  (Figure 3) contains four resonances in an approximate 4:8:4:1 integral ratio at  $\delta_1 = -1713$ ,  $\delta_2 = -1049$ ,  $\delta_3 = -1010$ , and  $\delta_4 = 228$  ppm, respectively. The number of peaks and their intensities are consistent with the  $D_{2d}$  structure of the cluster with four different Sn environments. The resonance at  $\delta_2$  has the highest peak intensity and is due to the eight equivalent Sn atoms bonded to the central Sn5 atom. The resonance with the lowest intensity,  $\delta_4$ , is assigned to Sn5. Since  $\delta_1$  and  $\delta_3$  have the same integrated area, it is not possible to assign these peaks based on intensity alone. However, previous studies<sup>18,19</sup> have shown that 4-coordinate capping Sn atoms in  $Sn_9$  polyhedra have anomalously downfield chemical shifts. As such, we tentatively assign the 4-coordinate Sn atoms (Sn2 and Sn9) to the downfield resonance  $\delta_3$ .

When the temperature is increased to  $-50\text{ }^\circ\text{C}$ , the line widths of the peaks at  $\delta_1$ ,  $\delta_2$ , and  $\delta_3$  increase, while the peak at  $\delta_4$  sharpens. At  $0\text{ }^\circ\text{C}$ ,  $\delta_1$ ,  $\delta_2$ , and  $\delta_3$  disappear into the baseline, while  $\delta_4$  remains

sharp (Supporting Information). At  $44\text{ }^\circ\text{C}$ , a time averaged exchange peak emerges at  $-1176$  ppm, while  $\delta_4$  is broadened but still clearly visible. The exchange peak is close to the expected weighted average of  $\delta_1$ ,  $\delta_2$ , and  $\delta_3$  ( $-1205$  ppm). Increasing the temperature to  $60\text{ }^\circ\text{C}$  results in the disappearance of resonance  $\delta_4$  and a shift of the exchange peak downfield to  $-1167$  ppm. The expected time average peak for total exchange is  $-1120$  ppm. The data suggest that an intramolecular exchange process is occurring at low temperature that does not involve the central Sn5 atom. At higher temperatures, global exchange is observed, indicating that all Sn atoms, including the unusually coordinated Sn5, are in rapid exchange on the NMR time scale. This surprising global atomic mobility is consistent with dynamic processes in single-focus clusters but is apparently operative in two-focus clusters, as well. Since the 8-coordinate Sn5 atom is more akin to solid-state Sn coordination environments, this process serves as a model for different exchange rates between surface and bulk atoms in NP systems.

**Acknowledgment.** This material is based upon work supported by the National Science Foundation under Grant No. 0401850.

**Supporting Information Available:** Variable temperature  $^{119}\text{Sn}$  NMR spectra. Crystallographic files for  $[K(2,2,2\text{-crypt})]_4[Ni_2Sn_{17}] \cdot en$  in .cif format. This material is available free of charge via the Internet at <http://pubs.acs.org>.

## References

- Niu, Y. H.; Crooks, R. M. *Compt. Rend. Chim.* **2003**, *6*, 1049–1059.
- Bonnemann, H.; Richards, R. M. *Eur. J. Inorg. Chem.* **2001**, 2455–2480.
- Wang, X. J.; Langetepe, T.; Persau, C.; Kang, B. S.; Sheldrick, G. M.; Fenske, D. *Angew. Chem., Int. Ed.* **2002**, *41*, 3818–3822.
- Ahlich, R.; Anson, C. E.; Clerac, R.; Fenske, D.; Rothenberger, A.; Sierka, M.; Wieber, S. *Eur. J. Inorg. Chem.* **2004**, 2933–2936.
- Fenske, D.; Persau, C.; Dehnen, S.; Anson, C. E. *Angew. Chem., Int. Ed.* **2004**, *43*, 305–309.
- Steiner, J.; Stosser, G.; Schnockel, H. *Angew. Chem., Int. Ed.* **2004**, *43*, 302–305.
- Fassler, T. F. *Coord. Chem. Rev.* **2001**, *215*, 347–377.
- Fassler, T. F. *Angew. Chem., Int. Ed.* **2001**, *40*, 4161–4165.
- Esenturk, E. N.; Eichhorn, B.; Fetting, J. Results to be published.
- Esenturk, E. N.; Fetting, J.; Lam, Y. F.; Eichhorn, B. *Angew. Chem., Int. Ed.* **2004**, *43*, 2132–2134.
- Esenturk, E. N.; Fetting, J.; Eichhorn, B. *Chem. Commun.* **2005**, 247–249.
- Goicoechea, J. M.; Sevov, S. C. *J. Am. Chem. Soc.* **2005**, *127*, 7676–7677.
- Goicoechea, J. M.; Sevov, S. C. *Angew. Chem., Int. Ed.* **2005**, *44*, 4026–4028.
- $K_4Sn_9$  (80 mg, 0.065 mmol) and 2,2,2-crypt (98 mg, 0.26 mmol) were dissolved in en (ca. 2 mL) and stirred for 5 min, yielding a dark red solution.  $Ni(COD)_2$  (18 mg, 0.065 mmol) was dissolved in toluene (ca. 1 mL), producing a pale yellow solution. The solutions were mixed, stirred for 4 h, and filtered to give a clear red–brown solution. After 10 days, dark red–brown pyramidal crystals were isolated from solution. Yield: ~25 mg (~20%). EDX Sn:Ni:K = 8.8:1:2.
- Kesanli, B.; Fetting, J.; Gardner, D. R.; Eichhorn, B. *J. Am. Chem. Soc.* **2002**, *124*, 4779–4786.
- Crystal data: monoclinic, space group  $I2/a$ ,  $a = 28.793(1)$  Å,  $b = 16.744(1)$  Å,  $c = 29.230(1)$  Å;  $V = 12663.4(11)$  Å<sup>3</sup>,  $\rho_{\text{calcd}} = 2.055\text{ g cm}^{-3}$ ,  $\mu(\text{Mo K}\alpha) = 3.765\text{ mm}^{-1}$ , 44 725 unique reflections for 915 parameters.  $GOF(F^2) = 1.072$ ,  $R1 = 0.0223$ ,  $wR2 = 0.0543$  for  $I > 2\sigma(I)$  and  $R1 = 0.0271$ ,  $wR2 = 0.0563$  for all data.
- Esenturk, E. N.; Fetting, J.; Eichhorn, B. *Polyhedron* **2005**, in press.
- Kesanli, B.; Fetting, J. C.; Gardner, D. R.; Eichhorn, B. W. *Chem.—Eur. J.* **2001**, 5277–5285.
- Campbell, J.; Mercier, H. P. A.; Holger, F.; Santry, D.; Dixon, D. A.; Schrobilgen, G. J. *Inorg. Chem.* **2002**, *41*, 86–107.
- Schiemenz, B.; Huttner, G. *Angew. Chem., Int. Ed. Engl.* **1993**, *32*, 297–298.
- Fassler, T. F.; Hoffmann, S.; Kronseder, C. Z. *Anorg. Allg. Chem.* **2001**, *627*, 2486–2492.
- Schrodt, C.; Weigend, F.; Ahlich, R. Z. *Anorg. Allg. Chem.* **2002**, *628*, 2478–2482.
- Moses, M. J.; Fetting, J. C.; Eichhorn, B. W. *Science* **2003**, *300*, 778–780.

JA055379+